DOI: 10.1002/chem.200801246

Supramolecular Chirality and Reversible Chiroptical Switching in New Chiral Liquid-Crystal Azopolymers

Joaquín Barberá,[b] Loris Giorgini,[a] Fabio Paris,[a] Elisabetta Salatelli,[a] Rosa M. Tejedor,[b] and Luigi Angiolini*[a]

Abstract: The synthesis of chiral liquid-crystalline polymers of well-controlled structure (linear and three-armed star-shaped) with distinct average chain lengths and low polydispersity was achieved by atom transfer radical polymerisation (ATRP) of a new optically active monomer (*S*)-4-[6-(2-methacryloyloxypropanoyloxy)hexyloxy)]-4′-ethoxyazobenzene [(*S*)-**ML6A**], containing the L-lactic residue of one absolute configuration in the side-chain. All the obtained polymeric samples, characterised by differential scanning calorimetry (DSC), X-ray diffraction (XRD) and polarised optical microscopy (POM), exhibit a smectic $A_{1/2}$ (fully interdigitated) liquid-crystalline phase and high cleaning points, with transition temperatures dependent on the average polymerisation degree and the macromolecular structure. The chirality originated at the molecular level by the asymmetric functionality of the L-lactic acid residue provides the polymers, in the smectic phase, of highly homogeneous conformations with a prevailing chirality related to the presence of H-aggregates having conformational dissymmetry of one prevailing screw-sense. By irradiating with circularly polarised light (CPL), it is possible to photomodulate the chiroptical properties of these intrinsically chiral polymeric thin films. Upon irradiation with left-handed CPL (*l*-CPL), the circular dichroism (CD) spectra of the films show enhancement of ellipticity and a net inversion of sign. The effect is reversible and the mirror image of the CD spectrum can be restored by pumping with right-handed CPL radiation (*r*-CPL). The results show the ability of *l*-CPL to invert the supramolecular chirality of the materials and demonstrate the essential role of azoaromatic aggregates.

Keywords: atom transfer radical polymerisation · chirality · liquid crystals · polymers · supramolecular chemistry

Introduction

Azobenzene-containing polymeric systems are well known for their photochromic properties related to the *trans-cis-trans* photoisomerisation of the azo-chromophore, and have been proposed for reversible data storage, signal modulation and switching.[1] The induction of helical polymers has been the subject of intense research, not only because of its potential applications in chiroptical switching, reversible optical storage,[2–6] chiral amplification[7] and chiral discrimination,[8] but also its possible occurrence at the early stages of life on earth.[9] Optically active polymers containing a chiral group and an azobenzene chromophore show a well-pronounced circular dichroism (CD) signal in the absorption region of azobenzene, demonstrating that the chiral centre induces a predominant helical screw-sense in the polymer both as film and in solution.[10–12] Recently, the fascinating possibility of inducing circular birefringence (optical activity) in nonchiral azobenzene-containing polymers by using circularly polarised light (CPL) has also been reported. This phenomenon was observed for the first time by Nikolova and co-workers in switches obtained by the direct irradiation of films of liquid-crystalline cyanoazobenzene polyesters.[13,14] Upon illumination with CPL at 488 nm, the films are provided with an unusually strong optical activity: right circularly polarised (*r*-CPL) radiation induces right-hand ro-

[a] Dr. L. Giorgini, Dr. F. Paris, Dr. E. Salatelli, Prof. L. Angiolini
Dipartimento di Chimica Industriale e dei Materiali and
INSTM UdR-Bologna, Università di Bologna
Viale Risorgimento 4, 40136 Bologna (Italy)
Fax: (+39) 051-209-3687
E-mail: luigi.angiolini@unibo.it

[b] Dr. J. Barberá, Dr. R. M. Tejedor
Química Orgánica
Instituto de Ciencia de Materiales de Aragón
Facultad de Ciencias
Universidad de Zaragoza-CSIC, Pedro Cerbuna 12
50009 Zaragoza (Spain)

Supporting information for this article is available on the WWW under http://dx.doi.org/10.1002/chem.200801246.

tation of the probe beam polarisation, the reverse being observed with left circularly polarised (*l*-CPL) pump light. In a first report,[13] the authors suggested that the observed effect may be initiated by a transfer of angular momentum from the CPL to the azobenzene chromophores and that the observed phenomena are related to the presence of liquid-crystalline (LC) ordering (smectic-A phase) in the polymer films prior to irradiation. Analogous results have been found for an amorphous cyanoazobenzene methylmethacrylate copolymer previously ordered by illumination with linearly polarised light.[15] In a further work, Nikolova et al. discovered a self-induced rotation of the azimuth of elliptically polarised light (EPL) on passing through films of photobirefringent azopolymers.[16] The EPL propagating through the sample was found to induce an optical axis that gradually rotates along the propagation direction, thus inducing a chiral orientation of the azobenzene chromophores with the same sense of rotation as that of the input light electric vector. The whole film assumes a chiral structure similar to that found in cholesteric liquid crystals with large pitch. The control of chirality with CPL on films of a smectic-A liquid-crystalline nitroazobenzene methyl-methacrylate polymer was also achieved by Natansohn and co-workers.[17] The authors found that, by irradiation with CPL at 514 nm, the initially achiral films became chiral and showed strong CD signals. The CD spectra of two different films, one irradiated with *r*-CPL and the other with *l*-CPL, exhibited opposite signs and were virtually mirror images of each other. In contrast, the amorphous films (not annealed) did not show any induced circular anisotropy, thus pointing out the essential role of the LC arrangement and suggesting that the original circular polarisation of the incoming light is made elliptical by the first layers of the smectic domains of the film. In this way, on the basis of the model proposed by Nikolova et al.,[16] the EPL radiation that propagates into the film produces a progressive rotation of the optical axis of each LC domain, resulting in a supramolecular helical arrangement of the smectic domains to form an organisation similar to a twisted grain boundary (TGB) phase.

According to Kim,[18] chirality can be induced also in amorphous epoxy-based side-chain azopolymers by illumination with one-handed EPL. In this context, we reported the first example of chiroptical switching with only *r*- or *l*-CPL of amorphous thin films of chiral polymethacrylates containing azoaromatic moieties in the side-chain, in the absence of preliminary alignment with linearly polarised (LP) light.[19–21] Hore et al. reported the observation of a selective circular Bragg reflection in the CD spectra of a nematic glassy thin film (100 nm thick) of a side-chain LC azopolymer irradiated with CPL, which was assigned to the structure produced by superposition of the forward-propagating wave and the back-reflected wave.[22] Although several mechanisms of the photoinduced chirality process in side-chain azobenzene-containing polymers have been proposed, the model based on a helical arrangement of aggregated chromophores in the side-chain[22] appears more realistic.

More recently, Tejedor et al. discussed the influence of LC structures and detected a circular Bragg reflection in thin films (200 nm) of achiral glassy nematic azopolymers,[23,24] but not in a homologous smectic one[23] irradiated with CPL of opposite sign.

To induce chirality in soft matter, two different structural levels must be mainly considered: the molecular and supramolecular. The first level is provided by the chirality of molecules, which is of configurational and conformational origin. The second level of chirality arises from the organisation of molecules with formation of a chiral superstructure by means of long-range positional and orientational orders of molecules.[25] As described above, several research groups have contributed to the experimental findings on chirality induced by CPL (or EPL) stimuli in achiral polymer systems with azobenzene moieties in their side-chains, but studies of liquid-crystalline polymers containing a chiral group of one absolute configuration and an azobenzene chromophore in the side-chain suitable to demonstrate CPL-induced chirality have not been reported. Furthermore, from all these investigations it appears that polymeric samples with a well-defined structure are needed for a better understanding of the structure–proprieties correlation; hence, derivates with a carefully selected molecular mass and low polydispersity are required.

This goal can be achieved easily by use of a controlled polymerisation procedure such as atom transfer radical polymerisation (ATRP). Herein, we compare the behaviour of linear and star-shaped liquid-crystalline polymers under irradiation with CPL aimed at a better understanding of the role played by the macromolecular structure in the photoinduction of chiral supramolecular arrangements. In particular, we have considered the polymers depicted in Scheme 1: a linear one, poly[(*S*)-4-[6-(2-methacryloyloxypropanoyloxy)hexyloxy)]-4′-ethoxyazobenzene] {poly[(*S*)-**ML6A**]-14}, and four related three-armed branched macromolecular derivatives with controlled average molecular weight, star[(*S*)-4-[6-(2-methacryloyloxypropanoyloxy)hexyloxy)]-4′-ethoxyazobenzene] {star[(*S*)-**ML6A**]-2 through star[(*S*)-**ML6A**]-24}, obtained by ATRP of the novel chiral monomer (*S*)-4-[6-(2-methacryloyloxypropanoyloxy)hexyloxy)]-4′-ethoxyazobenzene [(*S*)-**ML6A**], containing the intrinsically chiral L-lactic acid residue suitable to affect the supramolecular organisation of the liquid-crystal phase. With the aim to investigate the structure–property relationships of these systems, they have been compared with the analogous polydisperse linear derivative poly[(*S*)-**ML6A**]-AIBN (Scheme 1) obtained by 2-2′-azobisisobutyronitrile (AIBN) free-radical polymerisation.

All these polymeric materials display LC behaviour and give glassy smectic thin films. The chiroptical properties of the films before and after irradiation with *r*-CPL and/or *l*-CPL were investigated in detail by CD spectroscopy and their dependence on the macromolecular structure is discussed.

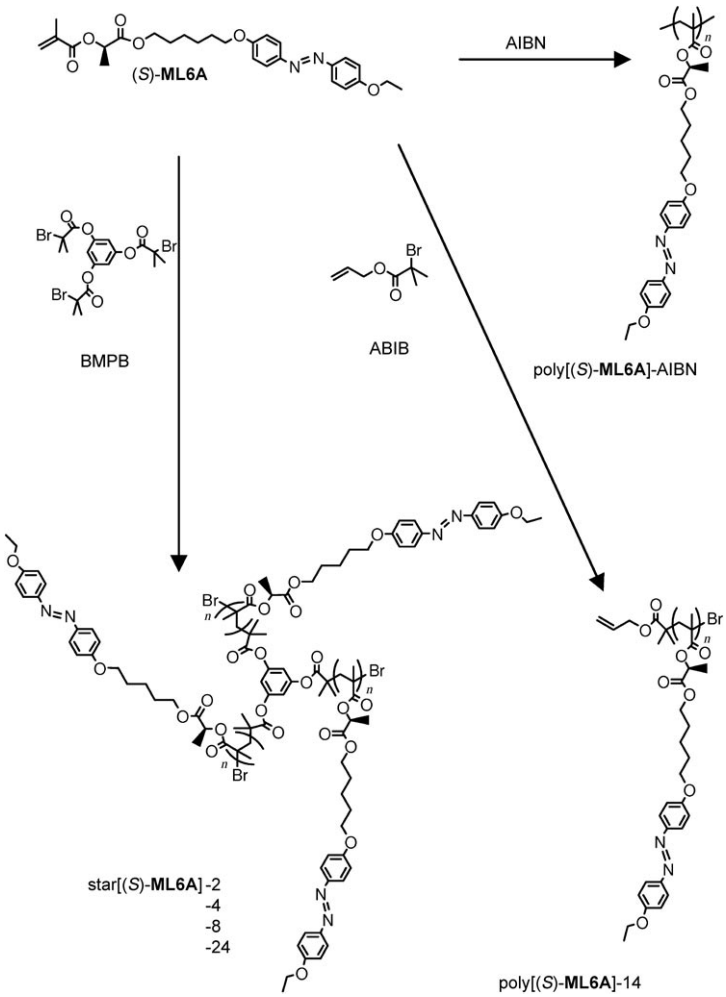

Scheme 1. Synthetic procedures and chemical structures of the investigated polymers.

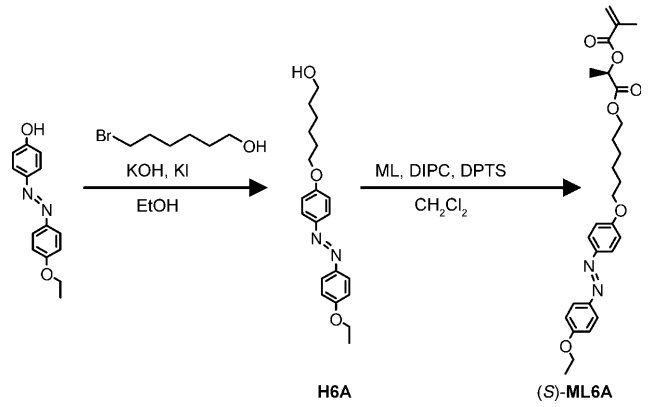

Scheme 2. Synthetic procedure for (*S*)-**ML6A**.

Results and Discussion

Synthesis and structural characterisation of monomer and polymeric derivatives: The key intermediate 4-(6-hydroxyhexyloxy)-4′-ethoxyazobenzene (**H6A**) was prepared under milder conditions and in higher yields than those reported in the literature[26,27] (see Experimental Section). The direct esterification of methacryloyl-L-lactic acid (ML) with **H6A** in the presence of *N*,*N*-diisopropylcarbodiimide (DIPC) and 4-(diphenylamino)piridinium 4-toluensulfonate (DPTS) as coupling agent and condensation activator, respectively,[28] gave (*S*)-**ML6A** with a total yield of 28% (Scheme 2).

This monomer was then homopolymerised in three different ways, that is, by free-radical polymerisation using AIBN as thermal initiator, and by ATRP polymerisation using allyl 2-bromo-2-methylpropionate (ABIB) as monofunctional initiator or 1,3,5-(2′-bromo-2′-methylpropionato)benzene (BMPB) as trifunctional initiator, thus affording linear and three-armed star-shaped polymers, respectively. The most relevant data of the syntheses are reported in Table 1.

Poly[(*S*)-**ML6A**]-AIBN, prepared by AIBN free-radical polymerisation over a long polymerisation time, was obtained in quite high yield (85%), with average molecular weight appreciably high and molecular-weight distribution typical of a free-radical-polymerisation process (Table 1). The polymers synthesised by ATRP show low values of polydispersity index ($\bar{M}_w/\bar{M}_n$) in accordance with this polymerisation method (Table 1). In the ^{1}H NMR spectra of the samples obtained by ATRP, the signals related to the aliphatic and aromatic protons of the initiators are overlapped with those of the repeating units in the case of the star derivatives (see Experimental Section and Supporting Information). For example, the star-shaped sample obtained at shorter reaction times {star[(*S*)-**ML6A**]-2} displays the resonances of the methylene and methyl groups bonded to the quaternary carbon atom bearing the terminal Br atom at 1.9 and 2.3 ppm, respectively (see Supporting Information). The living character of the polymerisation is confirmed by ^{13}C NMR spectra, which display signals related to the quaternary carbon atom bonded to Br at δ 58.0 ppm and to the methyl and methylene carbon atoms of the growing chain end-group at 27.5 and 38.9 ppm, respectively. An analysis of

Table 1. Characterisation data of polymeric derivatives.

Sample	Reaction time [h]	Yield[a] [%]	$\bar{M}_{n,th}$[b]	$\bar{M}_{n,SEC}$[c]	$\bar{M}_w/\bar{M}_n$	$[\alpha]_D^{25}$	$[\Phi]_D^{25}$[d]
(*S*)-**ML6A**	–	–	–	–	–	−4.0	−17.1
poly[(*S*)-**ML6A**]-AIBN	72	85	–	15400	1.54	−26.9	−115.3
poly[(*S*)-**ML6A**]-14	14	37	26700	13900	1.19	−27.6	−118.3
star[(*S*)-**ML6A**]-2	2	10	7800	8000	1.22	−26.8	−114.8
star[(*S*)-**ML6A**]-4	4	14	10900	11400	1.20	−27.0	−115.7
star[(*S*)-**ML6A**]-8	8	35	18700	19000	1.16	−27.8	−119.1
star[(*S*)-**ML6A**]-24	24	48	35600	27600	1.15	−28.5	−122.1

[a] Calculated as (g of polymer/g of monomer) × 100. [b] $\bar{M}_{n,th}$ calculated by using Equation (1). [c] Determined by SEC in THF at 25 °C. [d] Molar optical rotation, calculated as $([\alpha]_D^{25} \times \frac{\bar{M}}{100})$, in which M represents the molecular weight of one repeating unit of poly[(*S*)-**ML6A**] or star[(*S*)-**ML6A**].

the yields and of the molecular weights of the star polymers obtained with different polymerisation times shows that the polymerisation rates followed effective first-order kinetics. Figure 1 shows a linear relationship between $\ln([M]_0/[M]_t)$ (in which $[M]_0$ and $[M]_t$ are the initial and at time t monomer concentrations, respectively) and the reaction time, indicating clear first-order kinetics of the polymerisation rate with respect to the monomer concentration, and a relatively constant concentration of the growing species throughout the process, also at relatively high conversion, thus proving the living character of the process.

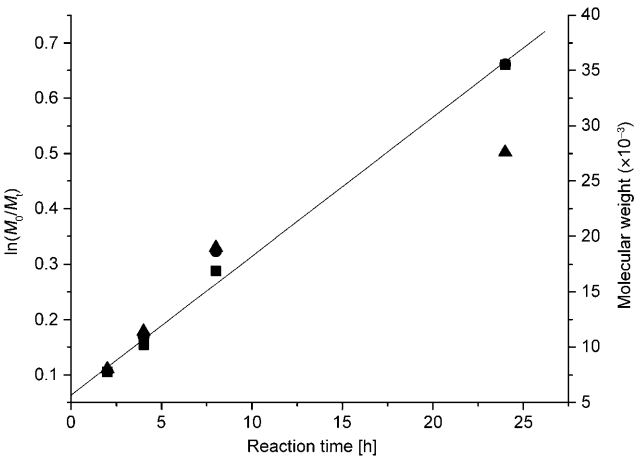

Figure 1. Evolution of $\ln([M]_0/[M]_t)$ (■) and of the number-average molecular weight determined by SEC in THF at 25 °C (▲) and calculated values (●) versus time in the ATRP of (*S*)-**ML6A** in THF for the star[(*S*)-**ML6A**] series.

The plot of the number-average molecular weight of the resulting star-shaped polymers as determined by the surface electroclinic effect (SEC) ($\bar{M}_{n,SEC}$) against monomer conversion (determined by collecting the unreacted monomer from the polymerisation mixture) is also shown in Figure 1. The theoretical values of $\bar{M}_n$ ($\bar{M}_{n,th}$), that are valid only in the absence of chain termination and transfer reactions, may be calculated by Equation (1):[29]

$$\bar{M}_{n,th} = \text{conversion} \times (M_{(S)\text{-}\mathbf{ML6A}}/M_{BMPB}) \times M_{W_{(S)\text{-}\mathbf{ML6A}}} + M_{W_{BMPB}} \quad (1)$$

in which $M_{(S)\text{-}\mathbf{ML6A}}$ and M_{BMPB} are the initial amounts in moles of monomer and trifunctional initiator, respectively, and $M_{W_{(S)\text{-}\mathbf{ML6A}}}$ and $M_{W_{BMPB}}$ their respective molecular weights. As reported in Figure 1, calculated and experimental (by SEC) values are coincident only at low values of monomer conversion, however, as the conversion increases, they diverge to an increasing extent. Such behaviour, previously reported for star-shaped chiral photochromic polymethacrylates,[30] cannot be ascribed to termination reactions taking place under the real polymerisation conditions, as proved by the low and almost constant values of $\bar{M}_w/\bar{M}_n$ (in the range 1.15–1.22), reported in Table 1, but rather to the particular molecular structure of multiarmed polymers. In fact, it is well known that star polymers have a smaller hydrodynamic volume relative to that of linear polystyrenes having the same polymerisation degree. As a consequence, SEC analysis gives underestimated molecular-weight values for star-shaped polymers if measured with reference to the usually adopted linear polystyrene standards.[31,32] However, the approximately linear correlation between $\bar{M}_{n,SEC}$ and time is indicative of the living character of the ATRP process, and SEC analysis proves to be useful in confirming that a steady increment of the average molecular weight with conversion has taken place, as shown by the chromatograms reported in Figure 2. In conclusion, all the instrumental characterisation

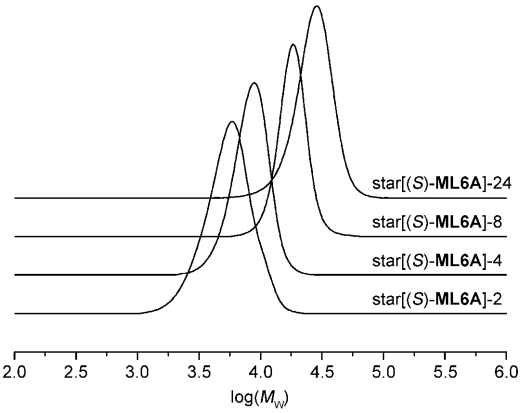

Figure 2. Normalised molecular-weight distributions of star[(*S*)-**ML6A**] polymers as determined by SEC in THF at 25 °C.

techniques confirm that three-armed star polymers with C_3 symmetry and varying molecular size have been successfully obtained. Each chain contains a bromine atom as end group that could be replaced through a variety of reactions leading either to end-functionalised polymers or used as the initiating site for the polymerisation of a different monomer to obtain novel and interesting star-shaped block copolymers as well as linear block copolymers, starting, for example, from poly[(*S*)-**ML6A**]-14.

POM, DSC and XRD characterisation: With the aim to study their LC properties, all polymeric derivatives were characterised by differential scanning calorimetry (DSC), polarised optical microscopy (POM) and X-ray diffraction (XRD). Phase-transition temperatures determined by DSC are summarised in Table 2: all the samples display on heating a glass-transition temperature (T_g) and a liquid-crystal phase with a consequent isotropisation temperature (T_i). The high enthalpy of isotropisation, about 9.6 J g^{-1}, is related to the presence of a typical smectic phase.

In all cases, on cooling, the latter transitions show a modest degree of supercooling (4–5 °C) and a stable, frozen liquid-crystal mesophase is achieved and maintained at room temperature.

Table 2. Thermal transitions[a] and mesomorphism determined by DSC, POM and XRD.

Sample	Thermal transition [°C]				
poly[(*S*)-**ML6A**]-AIBN	G	53	$SmA_{1/2}$	129	I
poly[(*S*)-**ML6A**]-14	G	56	$SmA_{1/2}$	129	I
star[(*S*)-**ML6A**]-2	G	48	$SmA_{1/2}$	114	I
star[(*S*)-**ML6A**]-4	G	49	$SmA_{1/2}$	117	I
star[(*S*)-**ML6A**]-8	G	59	$SmA_{1/2}$	132	I
star[(*S*)-**ML6A**]-24	G	61	$SmA_{1/2}$	133	I

[a] Obtained from the second heating DSC thermal cycle in nitrogen atmosphere (10 °C min^{-1}).

XRD studies were carried out at variable temperature on some representative compounds such as poly[(*S*)-**ML6A**]-14, star[(*S*)-**ML6A**]-2 and star[(*S*)-**ML6A**]-24. Firstly, X-ray patterns were recorded at room temperature on the above samples annealed for two hours 40 °C above the T_g, in order to develop the mesophase. Patterns were also taken at variable temperatures on virgin and unannealed samples. Finally, these compounds were mechanically aligned with the aim to obtain oriented patterns. The diffractograms of poly[(*S*)-**ML6A**]-14 under these several physical conditions are reported in the Supporting Information. In all cases the diffractograms are qualitatively very similar: all of them display a sharp Bragg reflection in the low-angle region and a diffuse, broad maximum in the high-angle region. This kind of pattern is characteristic of a liquid-crystal phase with a layered structure and confirms that the mesophase order exists at room temperature and is stable at high temperatures. The high-angle diffuse halo corresponds roughly to a mean distance of 4.4 Å and is associated with the liquid-like lateral interactions of the azoaromatic mesogenic groups. The measured spacing, deduced by applying Bragg's law to the low-angle reflection, is very close to 16 Å in all cases, regardless of the compound examined, the conditions of temperature and the thermal treatment (see Supporting Information). The predicted length of the mesogenic moiety calculated from Dreiding stereomodels, assuming a fully extended conformation of the hydrocarbon chains, is 31 Å (33 Å including the methacrylate group). Therefore, it appears that the observed low-angle maximum corresponds to the second order (d_{002}) reflection and the actual layer spacing is close to 32 Å, which is comparable to the value expected for a SmA arrangement of the mesogenic monomers. The fact that the first order (d_{001}) reflection is not visible must arise from the presence of a period $d/2$ in the projection of the electron-density profile along the normal to the layers. This phenomenon has been described for other side-chain LC polymers and is accounted for by the confinement of the polymeric backbones in a thin sublayer perpendicular to the director, so that the polymeric backbones produce an electron-density maximum comparable to that of the mesogenic cores.[33] These features are consistent with a fully interdigitated smectic A ($SmA_{1/2}$) mesophase (Figure 3). The absence of significant differences in layer periodicity by changing the macromolecular shape or the average molecular weight indicates that the same structural model is valid for all the samples, both with a linear polymeric backbone and a star-like arrangement.

Finally, mechanically aligned samples of poly[(*S*)-**ML6A**]-14 and star[(*S*)-**ML6A**]-24 were obtained by shearing the

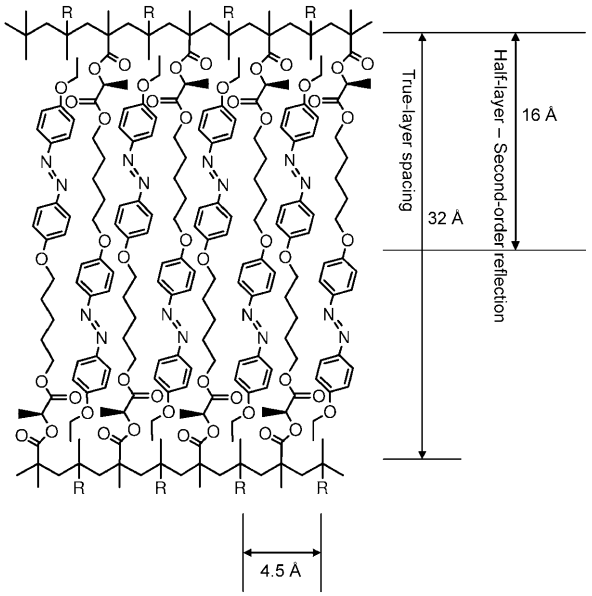

Figure 3. Smectic layer spacings of a fully interdigitated side-chain chromophoric configuration determined by XRD (R = chromophoric moieties located in the side-chain outside the layer).

samples on the capillary wall with a metal rod at a temperature at which the mesophase is fluid. Oriented patterns were obtained if the samples submitted to this treatment were irradiated at room temperature (see Supporting Information). In the resulting patterns the low-angle reflection appears as a pair of sharp spots aligned along the direction perpendicular to the shearing, whereas the high-angle halo becomes a pair of diffuse crescents centred in the shearing direction.

These features indicate that the smectic planes are oriented along the stretching direction with the mesogenic units oriented perpendicular to that direction. This behaviour is common for side-chain LC polymers. An accurate analysis of the nature of this mesophase was achieved by the observation of their typical optical texture by POM in analogy with previous studies on similar azopolymers.[34] All the samples, during the heating/cooling process, show textures that indicate the presence of macrodomains with a SmA phase, as shown, for example, for poly[(*S*)-**ML6A**]-14 in Figure 4. In particular, the thin film slowly cooled from the isotropic melt at 128 °C shows small drops of birefringent mesophases separating from the melt (Figure 4a) that develop after shearing and annealing at 110 °C for 48 h into cylindrical LC domains on an homeotropic background (Figure 4b). A polymeric film after isotropisation and annealing at 120 °C develops a typical cylindrical conicofocal texture like a SmA phase (Figure 4c).

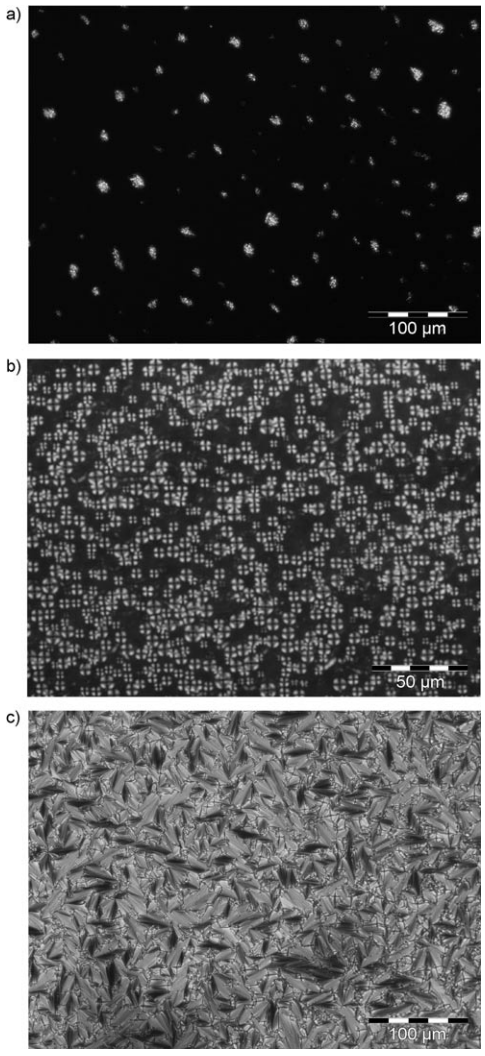

Figure 4. POM microphotographs of poly[(*S*)-**ML6A**]-14 (sample prepared between two glasses) a) at 128 °C upon cooling from the isotropic liquid, b) thin film annealed for 48 h at 110 °C after isotropisation and shear and c) thin film annealed for 24 h at 120 °C after isotropisation.

UV-visible spectra and chiroptical properties in solution: The UV-visible absorption spectra (Figure 5) in $CHCl_3$ solution of all the investigated linear and star polymers, as well as the monomer (*S*)-**ML6A**, exhibit, in the 250–550 nm spectral region, two bands related to the $n\rightarrow\pi^*$ and $\pi\rightarrow\pi^*$ electronic transitions of the *trans*-azobenzene chromophore with maxima centred at about 440 nm ($\varepsilon\cong1500\,L\,mol^{-1}\,cm^{-1}$) and 360 nm ($\varepsilon\cong28000\,L\,mol^{-1}\,cm^{-1}$), respectively,[35] appearing, within the limits of experimental error, qualitatively and quantitatively independent from molecular structure and polymerisation degree. The UV spectra do not exhibit any variation on passing from the monomer to the polymer, indicating the substantial absence of electrostatic dipole–dipole interactions between neighbouring aromatic moieties, the symmetry of the absorption band at 360 nm providing evidence that the azoaromatic chromophores are essentially isolated in solution. The monomer and all high-molecular-weight samples in the *trans* configuration are optically active in chloroform solution at the sodium D-line (Table 1). Indeed, the macromolecules investigated display molar optical-rotatory powers $[\alpha]_D^{25}$ for repeating units constantly around −28, seven times larger than that of (*S*)-**ML6A** ($[\alpha]_D^{25}=-4.0$), thus suggesting that the macromolecules are characterised by an appreciable conformational chirality.

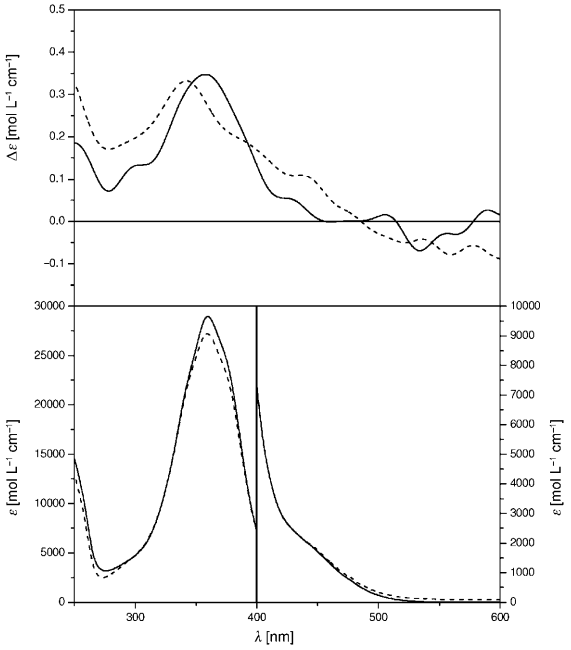

Figure 5. CD (top) and UV/Vis (bottom) spectra of (*S*)-**ML6A** (——) and poly[(*S*)-**ML6A**]-14 (– – –) in $CHCl_3$.

The CD spectrum of (*S*)-**ML6A** in chloroform solution (Figure 5) displays one weak positive dichroic absorption with maximum at 360 nm ($\Delta\varepsilon\approx+0.35\,L\,mol^{-1}\,cm^{-1}$), strictly related to the UV-visible absorption maximum connected with the $\pi\rightarrow\pi^*$ electronic transition. Similarly, the CD spectra of the polymeric samples in solution exhibit in the spectral region related to the $\pi\rightarrow\pi^*$ electronic transition only one positive dichroic band centred at about 350–360 nm ($\Delta\varepsilon\approx+0.2\,L\,mol^{-1}\,cm^{-1}$), in close correspondence with the UV absorption (Figure 5) and related to isolated chromophores. This is in a similar manner as the monomeric compound, with no influence by the average molecular-weight value and macromolecular shape, in agreement with the specific optical-rotatory powers (Table 1).

This behaviour is different from that reported in the literature for chiral, rigid methacrylic amorphous polymers that exhibit an increase in optical activity as molecular weight increases,[36] or on passing from linear to star-shaped structures.[30] The contribution to the overall optical activity in solution by the conformational dissymmetry of liquid-crystal polymeric derivatives, characterised by longer and flexible aliphatic spacer between the main-chain and the azoaromatic chromophore, thus appears of limited extent, as suggested

also by the specific optical-rotatory power at the sodium D-line.

UV-visible spectra and chiroptical properties in thin film: The UV-visible spectra and chiroptical properties of the synthesised polymers were investigated also in the solid state, as thin films prepared by casting from dichloromethane solution over clean slides of fused silica. By inspection with POM, the virgin films at room temperature appear optically isotropic: neither birefringence nor scattering being observed.

The main UV-visible data of relevant polymeric samples are collected in Table 3 and the absorption spectra of poly[(*S*)-**ML6A**]-14 in the solid state are reported as an example in Figure 6a: in addition to the typical $\pi\rightarrow\pi^*$ and $n\rightarrow\pi^*$ electronic transitions of the azoaromatic chromophore centred at around 357 and 440 nm, respectively, an additional band at around 248 nm, associated with the $\pi\rightarrow\pi^*$ transition of the single aromatic ring, is present.

The absorption band of the $\pi\rightarrow\pi^*$ transition in the virgin films appears broader with respect to the spectra in solution, with two additional shoulders at 340 and 380 nm, related respectively to the formation of H- (blue-shift) and J-like (red-shift) aggregates[37] imposed by the structural constraints of the macromolecules in the solid state. The relatively high absorbance of the transition at 340 nm indicates a high concentration of H aggregates in the amorphous solid state.

To develop the mesophase, a thermal treatment consisting of heating above the clearing-point temperature (T_i) for 5 min followed by annealing for 15 min at a temperature reduced by a factor of about 0.7 (T_{anneal}/T_i) was carried out.

The annealed film of poly[(*S*)-**ML6A**]-14 displays broader, less intense absorption bands (Figure 6a and Table 3) and produces LC domains as observed by POM. The main absorption band is characterised by a small bathochromic shift of the $\pi\rightarrow\pi^*$ azoaromatic absorption maximum to 362 nm. In addition, the shoulders related to the H- and J-aggregates located around 340 and 380 nm, increase relatively in importance. This can be related to development of aggregates and thus to more ordered dipolar intra- and interchain interactions that the chromophores experience in the $SmA_{1/2}$ phase (Figure 3) relative to the solution and the amorphous solid state.

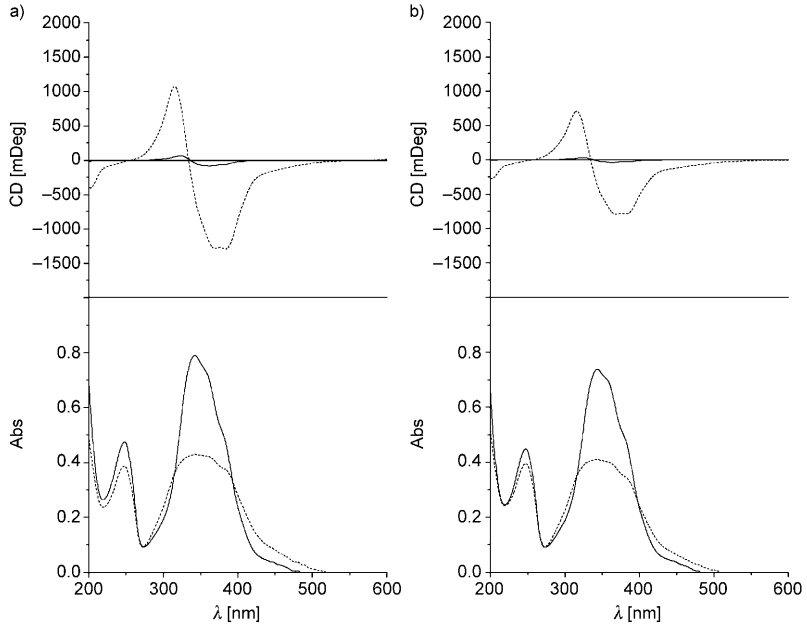

Figure 6. CD (top) and UV/Vis (bottom) spectra of a thin film of a) poly[(*S*)-**ML6A**]-14 and b) star[(*S*)-**ML6A**]-24 in the virgin state (——) and after isotropisation and annealing at 90 °C for 15 minutes (– – –).

Table 3. UV/Vis data of the investigated compounds in $CHCl_3$ solution and as thin films after different treatments.

Sample		$\lambda^{\phi\rightarrow\phi^*}$[a]	$\lambda^{\pi\rightarrow\pi^*}$[a]	$\lambda^{H\text{-agg.}}$[a,b]	$\lambda^{J\text{-agg.}}$[a,b]	$\lambda^{n\rightarrow\pi^*}$[a,b]
(*S*)-**ML6A**	solution	–[c]	360	–	–	440
poly[(*S*)-**ML6A**]-14	solution	–[c]	360	–	–	440
star[(*S*)-**ML6A**]-24	solution	–[c]	360	–	–	440
poly[(*S*)-**ML6A**]-14	virgin film	248	357	340	380	440
poly[(*S*)-**ML6A**]-14	annealed film	248	362	340	385	440
poly[(*S*)-**ML6A**]-14	irradiated film	248	360	345	385	440
star[(*S*)-**ML6A**]-24	virgin film	248	360	340	378	440
star[(*S*)-**ML6A**]-24	annealed film	248	360	340	380	440
star[(*S*)-**ML6A**]-24	irradiated film	248	360	344	385	440

[a] Wavelength of maximum absorbance in nm. [b] Shoulder. [c] Not observed due to solvent cut-off.

In particular, the decrease in absorbance of the $\pi\rightarrow\pi^*$ transition can be attributed to aggregation of the azobenzene fragments possessing elevated anisotropy,[38,39] whereas the $\pi\rightarrow\pi^*$ band at 248 nm of the single aromatic ring, not influenced by orientation, remains substantially unaffected. Finally, the increase in absorbance at wavelengths over 400 nm can be mainly associated with the light scattering due to formation of the birefringent domains of the liquid-crystal phase after annealing.

By comparing several CD spectra recorded at different film positions and rotated around the light beam direction it was also confirmed that the contribution of linear dichroism and linear birefringence to the CD spectra of the polymeric films is negligible.

The CD spectrum of a fresh film of poly[(*S*)-**ML6A**]-14 (Fig-

ure 6a) exhibits two relatively intense dichroic signals of opposite sign and similar intensity, connected to the $\pi\rightarrow\pi^*$ electronic transitions of the azoaromatic chromophores, with a crossover point at around 335 nm, close to the UV maximum absorption. This behaviour is typical of exciton splitting determined by cooperative dipole–dipole interactions between neighbouring side-chain azobenzene chromophores arranged in a mutual chiral geometry of one prevailing handedness.[4,36,40,41] Significantly, the CD spectrum of the same sample in dilute solution (Figure 5) displays only one weak positive dichroic signal at 360 nm, indicative of the absence in solution of chiral chromophore aggregates.

The thermal annealing strongly affects the chiroptical properties of the film (Figure 6a). Upon prolonged heating, a strong enhancement of CD signals takes place, and the ellipticity values become much more intense than those observed before annealing.

The crossover point of the couplets in the solid state appears blue-shifted with respect to the UV maximum absorbance (ellipticity = 0 at around 335 nm compared to a UV λ_{max} at 360 nm). Because the negative band appears of higher intensity, and close to the electronic transition wavelength associated with chiral H-aggregates (340 nm), the CD spectrum can be interpreted as originating from the overlapping of a exciton-splitted CD band given by the H-aggregates with a negative CD band having its maximum at 385 nm, corresponding to the maximum absorbance of J-aggregated chromophores, differently sensitive to the chiral geometry of the material.[23]

The UV-visible and CD spectra of star polymers of comparable thickness appear essentially similar to those of poly[(*S*)-**ML6A**]-14, as shown, for example, in Figure 6b for star[(*S*)-**ML6A**]-24. The star-shaped polymers as native films, as well as in the LC state, exhibit CD couplets with crossover points centred at 340 and 332 nm, respectively, of the same sign and shape as the related linear derivatives, but always less intense at equal film thickness.

From the CD spectra it can be clearly seen how branching affects the chirality of the system: the films of star[(*S*)-**ML6A**]-24 always exhibit a lower optical-rotation power than those of poly[(*S*)-**ML6A**]-14, thus suggesting that chirality is related in a certain way to the main-chain conformational order and/or to supramolecular liquid-crystalline organisation. A less ordered LC phase in the star-shaped derivatives could originate from the stiffness of the rigid central unit that creates defects in the LC supramolecular conformation. In any case, the above findings suggest that similar conformational arrangements with a prevailing chirality are assumed both in the amorphous and particularly in the LC phase, regardless of the molecular structure.

It is generally accepted that chirality is induced in these materials as a consequence of chiral interchromophoric interactions, however, short-range chromophoric aggregates in liquid-crystal arrangements could not be the only factor responsible for the remarkable amplification of chirality that is observed. Examples of amorphous azopolymeric systems, in which the chirality is related to the presence of chromophores aggregated in a mutual chiral arrangement, are reported in the literature, but these systems display lower optical-rotation values.[30,36,41]

In the present case, the presence of exciton couplets and surprisingly high ellipticity (up to 9000 mdeg μm^{-1} at 361 nm, Figure 6a) are quite noticeable for a normal smectic A phase with uniaxial symmetry and hence, lacking of any kind of supramolecular chirality. Consequently, the high chiroptical properties observed could suggest the presence of a chiral liquid-crystal phase similar to a planar twist-grain-boundary (TGB) phase or Sm-A* phases, reported only when chiral mesogens with high helical twisting power are present.[42,43] However, POM observation of thick films, as mentioned above, clearly suggests the presence of a normal smectic A phase. In the SmA phase, in which the chromophoric molecules are arranged perpendicular to the layer planes, the mesogenic moieties cannot adopt a supramolecular helical structure perpendicular to the layers. It can only occur parallel to the layers and only for systems with a strong twisting power. Therefore, a helical superstructure is only possible if screw dislocations punctuate the layers, giving rise to the so-called twisted-grain-boundary A phase (TGBA).[44,45] In the present case the formation of this particular mesophase appears highly improbable.

Moreover, thin films of chiral smectic A liquid crystals possessing high chirality due to the surface electroclinic effect (SEC) that induce in the film a chiral smectic C phase are reported in literature: the polar interaction between the glass wall and the LC material induces a polarisation resulting in a chiral reorientation of the LC director near the surface.[46,47]

It was not possible to obtain further information by XRD and polarised optical microscopy (texture analysis) regarding the molecular arrangement in these thin films (100–200 nm) as thicker film samples are required and the behaviour may be different when compared to the thin films investigated here.

Photoinduced switching of supramolecular chirality: Annealed thin films of poly[(*S*)-**ML6A**]-14 and star[(*S*)-**ML6A**]-24 of thickness about 140 nm in the glassy liquid-crystal state were irradiated with *r*-CPL and *l*-CPL, respectively, with an Ar^+ laser (power = 20 mW cm^{-2}) at 488 nm for 30 min. The UV-visible spectra of irradiated polymers are similar to those of annealed corresponding films (Table 3 and Figure 7). These results suggest that the dipolar azoaromatic aggregations (H- and J-aggregates) in the liquid-crystalline phase remain substantially unaffected by CPL irradiation.

Upon irradiation of poly[(*S*)-**ML6A**]-14 with *r*-CPL, the CD spectrum displays a net inversion of sign as well as a relevant amplification of chirality, particularly evident for the dichroic bands associated with the $\pi\rightarrow\pi^*$ azoaromatic electronic transition (see, for example, Figure 7).

According to the chiral exciton-coupling rules,[48] this behaviour suggests that *r*-CPL induces a right-handed screw-sense of coupled neighbouring azobenzene chromophores.

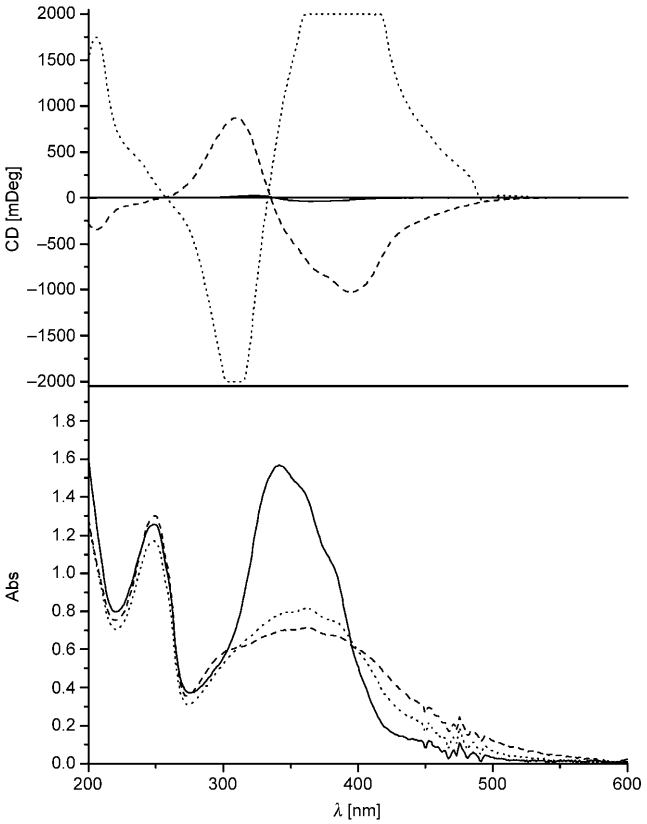

Figure 7. CD (top) and UV/Vis (bottom) spectra of a thin film of poly[(*S*)-**ML6A**]-14 in the virgin state (——), in smectic phase (– – –) and after irradiation with *r*-CPL at 488 nm for 30 min (•••••).

The CD spectra of this polymer after a cycle of illumination with *r*-CPL and *l*-CPL are presented in Figure 8. In all cases, no linear dichroism was observed before and after irradiation by comparing several CD spectra recorded at different angles around the incident light beam.

Similar results, but with lower ellipticity values, were also obtained from star[(*S*)-**ML6A**]-24 (Figure 8). One negative Cotton effect, with the same crossover wavelength (333 nm) as the non-irradiated film (334 nm) but which changes alternatively the sign in the 250–600 nm spectral region, was obtained with both the investigated polymers. The observed effects are reversible: when the handedness of the pump beam was switched from right to left and the irradiation performed on the same illuminated region for 30 min, similar and opposite CD spectra of poly[(*S*)-**ML6A**]-14 and star[(*S*)-**ML6A**]-24 were obtained (Figure 8).

The resulting spectra actually appear as mirror images of each other both for linear and star-shaped samples. Again, the CD spectra of the linear polymer display higher ellipticity values than the CD spectra of the star one.

The irradiation with *l*-CPL of another annealed film of poly[(*S*)-**ML6A**]-14 afforded also an induced optical activity of similar magnitude to that observed after irradiation with *r*-CPL, but of opposite sign.

As a first conclusion, the photoinduced experiments suggest that *r*-CPL induces right-handed supramolecular chirality of the materials, which can be erased and reinscribed with *l*-CPL, as reported elsewhere for other smectic, achiral azopolymers.[17,24] However, the induced circular anisotropy has to be erased in the latter case by heating the irradiated samples to the isotropisation temperature.

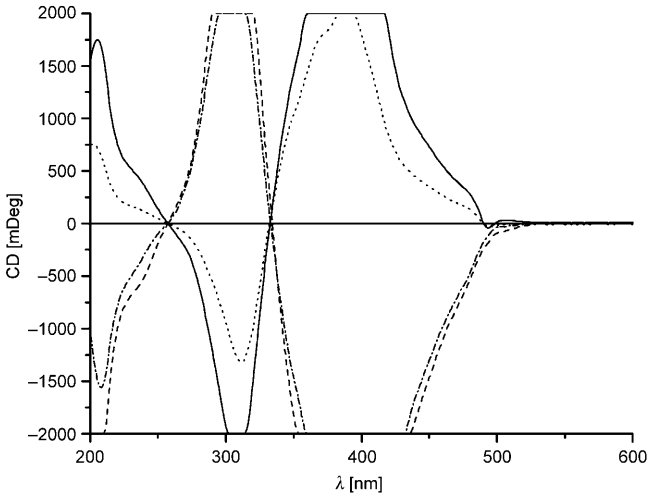

Figure 8. CD spectra of films of poly[(*S*)-**ML6A**]-14 irradiated with *r*-CPL (——) or *l*-CPL (– – –), and star[(*S*)-**ML6A**]-24 irradiated with *r*-CPL (•••••) or *l*-CPL (–•–•) for 30 min after isotropisation and annealing at 90 °C for 15 min.

The observed phenomena appear to be related to the induction of chirality by irradiation with CPL of achiral azobenzene-containing polymers reported by Nikolova,[13,15] Natansohn,[17] Sourisseau[49] and Tejedor,[23,24] even though the measured absolute ellipticity of our samples, normalised to film thickness, is of considerably higher magnitude. Indeed, in our case, an intrinsic chirality of the samples related to optical activity of the L-lactic acid residue interposed between the azo-chromophores and the polymer backbone is present, and the chiral geometry of the mesogenic aggregates in the annealed films gives rise to thermodynamically stable and unusual chiral LC phases with a predominant helical conformation, as previously reported when chiral mesogens are present.[42,43] These observations reveal that the photoinduced chirality in liquid-crystal polymers is more efficiently achieved when dissymmetric groups and chiral LC phases are present.

The mechanism of reversible chiroptical inversion induced by CPL radiation is not well understood. In any case, for the investigated polymers, it appears to be related to a preliminary chiral supramolecular ordering of the azobenzene moieties, as demonstrated in our experiments. In fact, no reproducible circular anisotropies can be photoinduced in the native films (not annealed), indicating the essential role of the liquid-crystalline arrangement. This also indicates that orientational preorganisation is required to obtain a controlled photomodulation of chirality.[15]

Moreover, the photoinduced change of chiroptical properties does not perturb the texture of the investigated polymeric films, as shown by POM analysis of the irradiated

area, before and after application of CPL (see Supporting Information).

Natansohn reported the photoinduction of a similar chiral supramolecular structure by illumination of an achiral azopolymer with CPL.[17] The results were attributed to the ability of the chiral CPL propagating through the film to produce a progressive rotation of the optical axis of each LC domain, resulting finally in a supramolecular helical arrangement of the smectic domains to form an organisation similar to a TGB phase.

In the case of the investigated polymers, it is reasonable to hypothesise that the LC phase in the annealed films assumes a helical supramolecular structure with a prevailing twist sense due to the thermodynamically favoured chiral interaction between neighbouring L-lactic-azoaromatic moieties, thus conferring a prevailing chirality to the material. Thus, the CPL should be able to alter this interaction between the chromophores and consequently the chiral supramolecular structure, so as to reverse the macroscopic chirality of the material without modifying the observable LC texture (see Supporting Information, Figure S4). This phenomenon would thus resemble the enantioselective CPL photochemical formation of optically active compounds from prochiral starting materials[50,51] and the CPL photoresolution of photochemically interconvertible enantiomers.[52,53]

In fact, it is known that chiral circularly polarised electromagnetic radiation is able to induce enantioselective conversion[54] and tends to align the azobenzene side groups along directions close to the light propagation.[14,55] It is possible that transfer of angular momentum from the CPL to the medium, as occurs when a CP photon is absorbed, induces a precession of the chromophores with a sense of rotation congruent to the sense of the CPL. This would mean that *l*-CPL induces a left-handed organisation of the azobenzene molecules, whereas *r*-CPL induces a right-handed one. In this way, the sign of the CD signals associated with the conformational aggregation of neighbouring chromophores can be inverted, as we have recently observed on the dimeric model derivative 2,4-dimethylglutaric acid bis-(*S*)-3-[1-(4′-nitro-4-azobenzene)pyrrolidine ester, corresponding to the smallest section of the polymeric chain in which side-chain interchromophore interactions are relevant.[41] Its CD spectrum shows an exciton couplet of strong amplitude which suggests that the chiral interactions between a couple of chromophores in solution are already important and that the optical activity of these materials should be substantially related to relatively short-chain sections with chromophoric aggregates having conformational dissymmetry of one prevailing screw-sense.

These observations are also supported by recent studies of photoinduced chirality onto a Bx liquid-crystalline phase of bent-shaped twin dimeric compounds, in which two alkoxyazobenzene groups linked together by a polymethylene spacer spontaneously segregate in chiral domains of the two possible dimeric conformers (racemic form).[56] Selective *r*- or *l*-CPL irradiation, as a method of photoresolution of enantiomers, interconverts the two native domains producing an enantiomeric excess of one of them, and as a result, a macroscopically measurable CD chirality related to the preferential screw-sense of the irradiating CPL.

All the aforementioned CD effects persist for at least one month at room temperature and are well reproducible. Clearly, for technological applications, the switching time would also be important. Further investigations of the dynamics of the observed phenomena are in progress.

Conclusions

Atom transfer radical polymerisation was successfully used to prepare a series of linear and three-armed star-shaped chiral liquid-crystalline polymers with different average molecular weights and low polydispersity. The liquid-crystalline behaviour of the synthesised polymers was confirmed by DSC measurements, with XRD and POM characterisations evidencing the presence of smectic $A_{1/2}$ phase in the material.

As assessed by UV-visible and CD spectroscopy, the macromolecules assume in the smectic phase highly homogeneous conformations with a prevailing chirality that appears related to the presence of H-aggregates, with conformational dissymmetry of one prevailing screw-sense due to thermodynamically favoured chiral interactions between neighbouring L-lactic-azoaromatic moieties. The CD spectra of the three-armed derivatives as solid thin films display similar behaviour, but lower ellipticity values than the CD spectra of linear derivatives with the same thickness. Actually, the area values of the CD signals indicate a chirality of the star polymer of about 2/3 of that of the linear polymer. The observed behaviour is due to the different structure of the polymeric samples and not to differences in the starting LC phase, as demonstrated by XRD. It thus appears that the branching of the macromolecular chain acts as a defect in the liquid-crystalline phase, leading to a less ordered supramolecular structure with lower chirality. In any case, the position of the CD exciton couplets is unaffected by the molecular structure of both the star and the linear polymer.

A larger chirality extent is photoinduced into the material by irradiation with *r*- or *l*-CPL, as seen by the enhanced intensity of the CD exciton couplets. Moreover, by changing the CPL handedness it is possible to switch between two configurationally opposite organisations of the macromolecules. This effect may be interpreted at the molecular level as a photoinduced inversion of the prevailing chiral conformation of the aggregated chromophores driven by a transfer of angular momentum from the CPL to the azobenzene chromophores.

To the best of our knowledge, these are the first examples of reversible chiroptical switching between two enantiomeric supramolecular structures obtained by irradiation with *l*- or *r*-CPL on highly chiral liquid-crystalline polymers. This feature makes these materials potentially suitable to be used as chiroptical switches and of interest in nanoscale technologies for the all-optical manipulation of information.

Experimental Section

Physico-chemical measurements: ^{1}H- and ^{13}C NMR spectra were obtained at RT in 5–10% $CDCl_3$ solutions, using a Varian NMR Gemini 300 spectrometer. Chemical shifts are given in ppm from tetramethylsilane (TMS) as the internal reference. ^{1}H NMR spectra were run at 300 MHz under the following experimental conditions: 24,000 data points, 4.5 kHz spectral width, 2.6 s acquisition time, 128 transients. ^{13}C NMR spectra were recorded at 75.5 MHz under full proton decoupling, under the following experimental conditions: 24,000 data points, 20 kHz spectral width, 0.6 s acquisition time, 64,000 transients. FTIR spectra were obtained by using a Perkin–Elmer 1750 spectrophotometer, equipped with an Epson Endeavour II data station, on samples prepared as KBr pellets. UV/Vis absorption spectra were recorded at 25 °C in the 700–250 nm spectral region by using a Perkin–Elmer Lambda 19 spectrophotometer in $CHCl_3$ solutions and with cell pathlengths of 0.1 cm. Concentrations of azobenzene chromophore of about 3×10^{-4} mol L^{-1} were used. Optical activity was measured at 25 °C in $CHCl_3$ solutions ($c\approx0.250$ g dL^{-1}) by using a Perkin–Elmer 341 digital polarimeter, equipped with a Toshiba sodium bulb, using a cell pathlength of 1 dm. Specific $\{[\alpha]_D^{25}\}$ and molar $\{[\Phi]_D^{25}\}$ rotation values at the sodium D-line are expressed as deg dm^{-1} g^{-1} cm^{-3} and deg dm^{-1} mol^{-1} dL, respectively. Circular dichroism (CD) spectra were obtained at 25 °C in $CHCl_3$ solutions by using a Jasco 810 A dichrograph, using the same pathlengths and solution concentrations as for the UV/Vis measurements. $\Delta\varepsilon$ values, expressed as L mol^{-1} cm^{-1}, were calculated from the following expression: $\Delta\varepsilon=[\Theta]/3300$, in which the molar ellipticity $[\Theta]$ in deg cm^{-2} dmol^{-1} refers to one azobenzene chromophore. Number-average molecular weights of the polymers ($\bar{M}_n$) and their polydispersity indexes ($\bar{M}_w/\bar{M}_n$) were determined in THF solution by SEC using the HPLC Lab Flow 2000 apparatus, equipped with an injector Rheodyne 7725i, a Phenomenex Phenogel 5-micron MXL column and a UV/Vis detector Linear Instrument model UVIS-200, working at 254 nm. The calibration curve for the MXL column was obtained by using monodisperse polystyrene standards in the range 800–35 000. Phase-transition temperatures were determined by differential scanning calorimetry (DSC) on a TA Instrument DSC 2920 modulated apparatus at a heating/cooling rate of 10 K min^{-1} under a nitrogen atmosphere on samples weighing 5–9 mg. T_g values were measured as the midpoint in the heat-capacity increase and the other thermal transitions were taken as the maximum of the transition peak. Texture observation of the liquid-crystalline behaviour was carried out with an Zeiss Axioscope2 polarising microscope equipped with a Nikon Coolpix E995 digital camera through crossed polarisers fitted with a Linkam THMS 600 hot stage. X-ray diffraction (XRD) studies were carried out using a Pinhole camera (Anton–Paar) operating with a point-focused Ni-filtered $Cu_{K\alpha}$ beam. The samples were held in Lindemann glass capillaries (1-mm diameter) and heated, when necessary, with a variable-temperature attachment. The diffraction patterns were collected on a flat photographic film perpendicular to the X-ray beam.

Polymer-film preparation, characterisation and irradiation with circularly polarised light: Thin films were prepared by casting solutions of the LC polymers in dichloromethane (0.4 mg into 200 μL of solvent) onto clean, fused silica slides and subsequently drying at 30 °C under vacuum over 24 h. The film thickness, measured by a Tencor P-10 profilometer, was in the range 150–300 nm, so as to give UV/Vis spectra with maximum absorbance values of between 0.7 and 1.5, depending on the procedure conditions. The obtained films were then heated above the clearing temperature (T_i) for 5 min and annealed for 15 min at lower temperature (T_{anneal}/T_i around 0.7). Then, the samples were placed on a metal block at 25 °C for 30 min to get a glassy liquid-crystalline phase. Annealed films were irradiated for 30 min with *l*-CPL or *r*-CPL, respectively, by 488 nm light of an Ar^+ laser (power 20 mW cm^{-2}). The UV/Vis and CD spectra of the native and illuminated films were recorded under the same instrumental conditions as the related solutions after having left the samples in the dark at RT for 30 min. To exclude any optical effect (linear dichroism and linear birefringence) due to anisotropy of orientation in the ordered systems, the polymeric films of both native and irradiated samples were placed in a rotating holder around the probe beam and UV/Vis and CD spectra were recorded every 60° without observing any difference in the spectra.

Materials: (*S*)-(−)-Methacryloyl-L-lactic (ML) acid $\{[\alpha]_D^{25}=-28.0$ ($c=1$, EtOH)} was synthesised as previously reported.[57] Methacryloyl chloride (Aldrich) was distilled under inert atmosphere, in the presence of traces of 2,6-di-*tert*-butyl-*p*-cresol as polymerisation inhibitor just before use. 4-Dimethylaminopyridinium 4-toluenesulfonate (DPTS) was prepared from 4-dimethylaminopyridine and 4-toluensulfonic acid as described.[28] 4-Hydroxy-4′-(ethoxy)-azobenzene was synthesised as previously described.[26,27] 2–2′-azobisisobutyronitrile (AIBN) was crystallised from methanol before use. THF and CH_2Cl_2 were purified and dried according to reported procedures[58] and stored under nitrogen. The trifunctional initiator 1,3,5-(2′-bromo-2′-methylpropionato)benzene (BMPB) was prepared as previously described.[59,60] (+)-L-Lactic acid (Aldrich), 1,3-diisopropylcarbodiimide (DIPC, Aldrich), 4-dimethylaminopyridine (Aldrich), the monofunctional initiator allyl 2-bromine 2-methylpropionate (ABIB) (Aldrich), 1,1,4,7,10,10-hexamethyltriethylenetetramine (HMTETA), copper bromide and all other reagents and solvents (Aldrich) were used as received.

4-(6-Hydroxyhexyloxy)-4′-ethoxyazobenzene [H6A]: This intermediate was prepared by following a different method than that reported.[26,27] 6-Chlorine hexanol (6.9 mL, 0.0496 mol) was added dropwise under vigorous stirring to a solution of 4-hydroxy-4′-(ethoxy)-azobenzene (6 g, 0.0248 mol), KOH (0.6 g, 0.011 mol) and KI (1.64 g, 0.0099 mol) in 96% ethanol (80 mL) at reflux. The reaction was followed by TLC (CH_2Cl_2/EtOAc 4:1) until the total conversion of 4-hydroxy-4′-(ethoxy)-azobenzene (48 h) was observed. The precipitated material was filtered off, the solvent volume reduced to 15 mL under vacuum, then aq 1% NaOH was added under vigorous stirring. The solid formed was filtered and crystallised twice with absolute ethanol to give a orange crystalline material (6.35 g, 77%). ^{1}H NMR ($CDCl_3$): $\delta=7.90$ (d, 4H; arom 2-H, 2′-H), 6.90 (d, 4H; arom 3-H, 3′-H), 4.15 (m, 4H; CH_3-CH_2-O, CH_2-CH_2-O), 3.65 (t, 2H; CH_2-OH), 1.85–1.40 ppm (m, 12H; CH_2-CH_2-CH_2-CH_2, CH_3-CH_2-O, O*H*); FTIR (KBr): $\tilde{\nu}=3308$ (ν_{OH}), 3069 (ν_{CH}, arom), 2978 and 2864 (ν_{CH}, aliph), 1600 and 1517 ($\nu_{C=C}$, arom), 1150 and 1111 (ν_{C-O} ether), 845 and 815 cm^{-1} (δ_{CH} 1,4 disubst. arom ring).

(*S*)-4-[6-(2-Methacryloyloxypropanoyloxy)hexyloxy)]-4′-ethoxyazobenzene [(*S*)-ML6A]: The monomer (*S*)-**ML6A** was prepared by esterification of methacryloyl-L-lactic acid (ML) with **H6A** in the presence of *N*,*N*-diisopropylcarbodiimide (DIPC) and DPTS, as coupling agent and condensation activator, respectively,[28] the reaction being described in detail as follows: a solution of ML (2.0 g, 0.0126 mol), 2,6-di-*tert*-butyl-*p*-cresol (0.05 g) as polymerisation inhibitor and **H6A** (4.34 g, 0.0126 mol) in 50 mL of anhydrous CH_2Cl_2 was placed in a 100-mL three-necked round-bottomed vessel and kept under dry nitrogen atmosphere. Then DPTS (3.64 g, 0.0126 mol) and DIPC (2.60 mL, 0.0168 mol) were successively added under magnetic stirring. The reaction mixture was left at RT for 72 h, the solid *N*,*N*-diisopropylurea thus formed filtered off and the liquid phase washed with several portions of aq 1 M HCl, aq 5% Na_2CO_3 and water, in that order. After drying the organic layer on anhydrous Na_2SO_4 and evaporation of the solvent under vacuum, the crude product was purified by column chromatography on silica gel (70–230 mesh) by using CH_2Cl_2 as eluent, and finally crystallised from methanol to give pure (*S*)-**ML6A** as a red-orange crystalline material (2.49 g, 41%). ^{1}H NMR ($CDCl_3$): $\delta=7.90$ (d, 4H; arom 2-H, 2′-H), 6.90 (d, 4H; arom 3-H, 3′-H), 6.20 and 5.60 (dd, 2H; CH_2=), 5.1 (m, 1H; C*H*-CH_3), 4.10 (m, 2H; CH_3-CH_2-O and 4H; CH_2-CH_2-O), 2.05 (s, 3H; CH_3-C=), 1.85–1.40 ppm (m, 14H; CH_2-CH_2-CH_2-CH_2, CH_3-CH_2-O, CH-CH_3); ^{13}C NMR ($CDCl_3$): $\delta=176,9$ (CO methacrylic), 171.1 (CO lactic ester), 161.7 and 161.6 (arom 4-C, 4′-C), 147.7 (arom 1-C, 1′-C), 136.1 (*C*=CH_2), 127.0 (CH_2=*C*), 125.0 (arom 2-C, 2′-C), 115.3 (arom 3-C, 3′-C), 69.6 (*C*H-CH_3), 68.7 (CH_2-CH_2-O-), 65.9 (CH_3-CH_2-O-), 64.4 (COO-CH_2-), 29.8, 29.1, 26.4, 26.3 (aliph spacer CH_2), 18.9 (C-CH_3), 17.7 (*C*H_3-CH), 15.4 ppm (*C*H_3-CH_2); FTIR (KBr): $\tilde{\nu}=3067$ (ν_{CH}, arom), 2993 and 2864 (ν_{CH}, aliph), 1738 ($\nu_{C=O}$ lactic ester), 1720 ($\nu_{C=O}$ methacrylic ester), 1638 ($\nu_{C=C}$ methacrylic), 1600 and 1517 ($\nu_{C=C}$, arom), 1150 and 1112 (ν_{C-O} ether), 845 and 815 cm^{-1} (δ_{CH} 1,4 disubst. arom ring).

Polymerisation of monomer (*S*)-ML6A: Several homopolymeric samples with different average molecular weights, polydispersity values and molecular structure were obtained from (*S*)-**ML6A** through three different synthetic methods as described below. Relevant data for the synthesised polymeric derivatives are reported in Table 1. All the products were characterised by FTIR, ^{1}H- and ^{13}C NMR.

Linear poly[(*S*)-ML6A]-AIBN: The reaction mixture [0.2 g of (*S*)-**ML6A**, 2% wt. of 2,2′-azoisobutyronitrile (AIBN) as free-radical initiator in 3 mL of dry THF] was introduced into a glass vial under nitrogen atmosphere, submitted to several freeze-thaw cycles and heated at 60°C for 72 h. The polymerisation was then stopped by pouring the mixture into a large excess (100 mL) of methanol, and the coagulated polymer filtered off. The solid product was redissolved in CH_2Cl_2, precipitated again into methanol and finally dried at 50°C under vacuum for several days to constant weight.

Linear poly[(*S*)-ML6A]-14 by ATRP: The homopolymerisation of (*S*)-**ML6A** was carried out in glass vials using ABIB as the linear monofunctional initiator, HMTETA as the ligand, Cu(I)Br as catalyst and dry THF as solvent [(*S*)-**ML6A**/THF 1/15 g mL^{-1}]. The reaction mixture [(*S*)-**ML6A**/ABIB/HMTETA/CuBr 50:1:1:1 by mol] was introduced into a glass vial under nitrogen atmosphere, submitted to several freeze–thaw cycles and heated at 60°C. To stop the polymerisation reaction, the vial was frozen after 14 h with liquid nitrogen and the obtained linear polymer purified by precipitation in a large excess of methanol (100 mL). The final purification of the product was achieved as described above.

Star[(*S*)-ML6A] series by ATRP: All homopolymerisations of (*S*)-**ML6A** were carried out in several glass vials using BMPB as the three-armed star-shaped trifunctional initiator, HMTETA as the ligand and Cu(I)Br as catalyst in dry THF [(*S*)-**ML6A**/THF = 1/15 g mL^{-1}]. The mixture [(*S*)-**ML6A**/BMPB/HMTETA/CuBr 150:1:3:3 by mol] was introduced into each vial under nitrogen atmosphere, submitted to several freeze–thaw cycles and heated at 60°C. To stop the polymerisation reaction, each vial was frozen in liquid nitrogen after reaction times ranging from 2 to 24 h, and the obtained polymeric products (star[(*S*)-**ML6A**]-2 through star[(*S*)-**ML6A**]-24) were purified as described above. As an example, the spectroscopic data for star[(*S*)-**ML6A**]-8, obtained after 8 h of reaction, are reported here: ^{1}H NMR ($CDCl_3$): $\delta = 7.90$ (d, 4H; arom 2-H, 2′-H), 6.90 (m, 3H; arom core and 4H; 3-H, 3′-H), 5.10–4.90 (m, 1H; C*H*-CH_3), 4.10–3.80 (m, 2H; CH_3-CH_2-O and 4H; CH_2-CH_2-O), 2.20 (CH_2-C-Br), 1.95 (m, 3H; CH_3-C-Br), 1.85–0.90 ppm (m, 19H; aliph spacer CH_2, CH_3-CH_2-O, CH-CH_3, backbone CH_3, CH_2 and 18H; C(CH3)2-COO); ^{13}C NMR ($CDCl_3$): $\delta = 176.9$ (CO methacrylic repeating unit), 171.1 (CO lactic ester), 167.8 (CO core), 161.7 and 161.6 (arom 4-C, 4′-C), 153.1 (C-O arom core), 147.6 (arom 1-C, 1′-C), 125.0 (arom 2-C, 2′-C), 115.3 (arom 3-C, 3′-C), 113.1 (arom *C*-H core), 70,0 (*C*H-CH_3), 68.7 (CH_2-*C*H_2-O-), 65.7 (CH_3-*C*H_2-O-), 64.4 (COO-*C*H_2-), 58.0 (*C*(CH_3)-Br), 54.2 (main-chain *C*-CH_2), 46.2 and 45.9 (main-chain *C*H_2-C), 42.2 (*C*(CH_3)$_2$-CH_2), 38.9 (*C*H_2-C(CH_3)-Br), 27.5 (C(*C*H_3)-Br), 29.8, 29.1, 26.5, 26.4 (aliph spacer CH_2), 23.2 (C(*C*H_3)$_2$-CH_2), 19.9 and 17.7 (main-chain CH_3), 17.7 (*C*H_3-CH), 15.4 ppm (*C*H_3-CH_2); FTIR (KBr): $\tilde{\nu} = 3069$ (ν_{CH}, arom), 2980 and 2865 (ν_{CH}, aliph), 1733 ($\nu_{C=O}$ lactic ester and $\nu_{C=O}$ main-chain methacrylic ester), 1598 and 1517 ($\nu_{C=C}$, arom), 1150 and 1111 (ν_{C-O} ether), 844 and 815 cm^{-1} (δ_{CH} 1,4 disubst. arom ring).

Acknowledgements

The financial support by MIUR (PRIN 2007), Consortium INSTM, University of Bologna (CLUSTERCAT-Strategic project 2006) and CICYT-FEDER (CTQ2006-15611-C02-01) is gratefully acknowledged.

[1] M. Irie, *Chem. Rev.* **2000**, *100*, 1683–1684.
[2] Y. Agata, M. Kobayashi, H. Kimura, M. Takeishi, *Polym. Int.* **2005**, *54*, 260–266.
[3] E. G. Nadal, J. Veciana, C. Rovira, D. Amabilino, *Adv. Mater.* **2005**, *17*, 2095–2098.
[4] L. Angiolini, T. Benelli, L. Giorgini, E. Salatelli, *Polymer* **2005**, *46*, 2424–2432.
[5] T. Kaneko, Y. Umeda, T. Yamamoto, M. Teraguchi, T. Aoki, *Macromolecules* **2005**, *38*, 9420–9426.
[6] B. L. Feringa, R. A. V. Delden, N. Koumura, E. M. Geertsema, *Chem. Rev.* **2000**, *100*, 1789–1816.
[7] Y. Oaki, H. Imai, *J. Am. Chem. Soc.* **2004**, *126*, 9271–9275.
[8] T. J. Wigglesworth, D. Sud, T. B. Norsten, V. S. Lekhi, N. R. Branda, *J. Am. Chem. Soc.* **2005**, *127*, 7272–7273.
[9] T. Kajitani, H. Masu, S. Kohmoto, M. Yamamoto, K. Yamaguchi, K. Kishikawa, *J. Am. Chem. Soc.* **2005**, *127*, 1124–1125.
[10] L. Angiolini, T. Benelli, L. Giorgini, E. Salatelli, R. Bozio, A. Dauru, D. Pedron, *Eur. Polym. J.* **2005**, *41*, 2045–2054.
[11] L. Angiolini, D. Caretti, L. Giorgini, E. Salatelli, *Macromol. Chem. Phys.* **2000**, *201*, 533–542.
[12] G. D. Jaycox, *J. Polym. Sci. Part A: Polym. Chem.* **2004**, *42*, 566–577.
[13] L. Nikolova, T. Todorov, M. Ivanov, F. Andruzzi, S. Hvilsted, P. S. Ramanujam, *Opt. Mater.* **1997**, *8*, 255–258.
[14] I. Nayadenova, L. Nikolova, P. S. Ramanujam, S. Hvilsted, *J. Opt. A: Pure Appl. Opt.* **1999**, *1*, 438–441.
[15] M. Ivanov, I. Nayadenova, T. Todorov, L. Nikolova, T. Petrova, N. Tomova, V. Dragostinova, *J. Mod. Opt.* **2000**, *47*, 861–867.
[16] L. Nikolova, L. Nedelchev, T. Todorov, T. Petrova, N. Tomova, V. Dragostinova, P. S. Ramanujam, S. Hvilsted, *Appl. Phys. Lett.* **2000**, *77*, 657–659.
[17] G. Iftime, F. L. Labarthet, A. Natansohn, P. Rochon, *J. Am. Chem. Soc.* **2000**, *122*, 12646–12650.
[18] M.-J. Kim, B.-G. Shin, J.-J. Kim, D.-Y. Kim, *J. Am. Chem. Soc.* **2002**, *124*, 3504–3505.
[19] L. Angiolini, R. Bozio, L. Giorgini, D. Pedron, A. Daurû, G. Turco, *Chem. Eur. J.* **2002**, *8*, 4241–4247.
[20] L. Angiolini, T. Benelli, R. Bozio, A. Dauru, L. Giorgini, D. Pedron, *Synth. Met.* **2003**, *139*, 743–746.
[21] L. Angiolini, L. Giorgini, R. Bozio, D. Pedron, *Synth. Met.* **2003**, *138*, 375–379.
[22] D. Hore, Y. Wu, A. Natansohn, P. Rochon, *J. App. Phys.* **2003**, *94*, 2162–2166.
[23] R. M. Tejedor, M. Millaruelo, L. Oriol, J. L. Serrano, R. Alcalá, F. J. Rodríguez, B. Villacampa, *J. Mater. Chem.* **2006**, *16*, 1674–1680.
[24] R. M. Tejedor, L. Oriol, J. L. Serrano, F. P. Ureña, J. J. L. González, *Adv. Func. Mater.* **2007**, *17*, 3486–3492.
[25] E. L. Eliel, S. H. Wilen, L. N. Mander, *Stereochemistry of Organic Compounds*, Wiley-VCH, New York, **1994**.
[26] D. Wolff, H. Cackovic, H. Krüger, J. Rübner, J. Springer, *Liq. Cryst.* **1993**, *14*, 917–928.
[27] A. S. Angeloni, D. Caretti, C. Carlini, E. Chiellini, G. Galli, A. Altomare, R. Solaro, M. Laus, *Liq. Cryst.* **1989**, *4*, 513–527.
[28] J. S. Moore, S. I. Stupp, *Macromolecules* **1990**, *23*, 65–70.
[29] X. Z. Wang, H. L. Zhang, D. C. Shi, J. F. Chen, X. Y. Wang, Q. F. Zhou, *Eur. Polym. J.* **2005**, 41, 933–940.
[30] L. Angiolini, T. Benelli, L. Giorgini, E. Salatelli, *Macromolecules* **2006**, *39*, 3731–3737.
[31] K. Matyjaszewski, P. J. Miller, J. Pyun, G. Kickelbick, S. Diamanti, *Macromolecules* **1999**, *32*, 6526–6535.
[32] S. Angot, K. S. Murthy, D. Taton, Y. Gnanou, *Macromolecules* **1998**, *31*, 7218–7225.
[33] P. Davidson, A. M. Levelut, M. F. Achard, F. Hardouin, *Liq. Cryst.* **1989**, *4*, 561–571.
[34] M. Kozlovsky, B. J. Jungnickel, H. Ehrenberg, *Macromolecules* **2005**, *38*, 2729–2738.
[35] H. H. Jaffé, M. Orchin, *Theory and Application of Ultraviolet Spectroscopy*, Wiley, New York, **1962**.
[36] L. Angiolini, T. Benelli, L. Giorgini, E. Salatelli, *Polymer* **2006**, *47*, 1875–1885.
[37] M. Shimomura, T. Kunitake, *J. Am. Chem. Soc.* **1987**, *109*, 5175–5183.
[38] J. G. Meier, R. Ruhmann, J. Stumpe, *Macromolecules* **2000**, *33*, 843–850.

[39] I. Zebger, M. Rutloh, U. Hoffmann, J. Stumpe, H. W. Siesler, S. Hvilsted, *Macromolecules* **2003**, *36*, 9373–9382.
[40] F. Ciardelli, C. Carlini, R. Solaro, A. Altomare, O. Pieroni, J. L. Houben, A. Fissi, *Pure Appl. Chem.* **1984**, *56*, 329–342.
[41] A. Painelli, F. Terenziani, L. Angiolini, T. Benelli, L. Giorgini, *Chem. Eur. J.* **2005**, *11*, 6053–6063.
[42] L. M. Blinov, M. Kozlovsky, G. Cipparrone, *Chem. Phys.* **1999**, *245*, 473–485.
[43] G. Srajer, R. Pindak, M. A. Waugh, J. W. Goodby, *Phys. Rev. Lett.* **1990**, *64*, 1545–1548.
[44] J. W. Goodby, *Struct. Bonding* **1999**, *95*, 83–147.
[45] A. C. Ribeiro, H. T. Nguyen, Y. Galerne, D. Guillon, *Liq. Cryst.* **2000**, *27*, 27–34.
[46] M. S. Spector, S. K. Prasad, B. T. Weslowski, R. D. Kamien, J. V. Selinger, B. R. Ratna, R. Shashidhar, *Phys. Rev. E* **2000**, *61*, 3977–3983.
[47] J. Xue, N. A. Clark, *Phys. Rev. E* **1990**, 64, 307–310.
[48] N. Berova, K. Nakanishi, R. W. Woody, *Circular Dichroism Principles and Applications*, Wiley-VCH, New York, **2000**.
[49] S. Pagès, F. Lagugné Labarthet, T. Buffeteau, C. Sourisseau, *Appl. Phys. B* **2002**, *75*, 541–548.
[50] T. Fujiwara, N. Nanba, K. Hamada, F. Toda, K. Tanaka, *J. Org. Chem.* **1990**, *55*, 4532–4537.
[51] A. Moradpour, J. F. Nicoud, G. Balavoine, H. Kagan, G. Tsoucaris, *J. Am. Chem. Soc.* **1971**, *93*, 2353–2354.
[52] K. S. Burnham, G. B. Schuster, *J. Am. Chem. Soc.* **1999**, *121*, 10245–10246.
[53] N. P. M. Huck, W. F. Jager, B. de Lange, B. L. Feringa, *Science* **1996**, *273*, 1686–1688.
[54] S. W. Choi, S. Kawauchi, N. Y. Ha, H. Takezoe, *Phys. Chem. Chem. Phys.* **2007**, *9*, 3671–3681.
[55] S. Sajti, A. Kerekes, M. Barabás, E. Lörincz, S. Hvilsted, P. S. Ramanujam, *Opt. Commun.* **2001**, *194*, 435–442.
[56] S. W. Choi, T. Izumi, Y. Hoshino, Y. Takanishi, K. Ishikawa, J. Watanabe, H. Takezoe, *Angew. Chem.* **2006**, *118*, 1410–1413; *Angew. Chem. Int. Ed.* **2006**, *45*, 1382–1385.
[57] V. A. Miller, R. R. Brown, E. B. Gienger, Jr., US 3067180, **1962**.
[58] D. D. Perrin, W. L. F. Amarego, D. R. Perrin, *Purification of Laboratory Chemicals*, Pergamon Press, Oxford, **1966**.
[59] D. M. Haddleton, C. Waterson, *Macromolecules* **1999**, *32*, 8732–8739.
[60] A. Carlmark, R. Vestberg, E. M. Jonsson, *Polymer* **2002**, *43*, 4237–4242.

Received: June 23, 2008
Published online: November 5, 2008

